Dalton Transactions

Cite this: *Dalton Trans.*, 2012, **41**, 12749

www.rsc.org/dalton

PAPER

Decavanadate, decaniobate, tungstate and molybdate interactions with sarcoplasmic reticulum Ca^{2+}-ATPase: quercetin prevents cysteine oxidation by vanadate but does not reverse ATPase inhibition

Gil Fraqueza,[a] Luís A. E. Batista de Carvalho,[b] M. Paula M. Marques,[c] Luisa Maia,[d] C. André Ohlin,[e] William H. Casey[f] and Manuel Aureliano*[g]

Received 26th July 2012, Accepted 23rd August 2012
DOI: 10.1039/c2dt31688a

Recently we demonstrated that the decavanadate (V_{10}) ion is a stronger Ca^{2+}-ATPase inhibitor than other oxometalates, such as the isoelectronic and isostructural decaniobate ion, and the tungstate and molybdate monomer ions, and that it binds to this protein with a 1 : 1 stoichiometry. The V_{10} interaction is not affected by any of the protein conformations that occur during the process of calcium translocation (*i.e.* E1, E1P, E2 and E2P) (Fraqueza *et al.*, *J. Inorg. Biochem.*, 2012). In the present study, we further explore this subject, and we can now show that the decaniobate ion, $[Nb_{10} = Nb_{10}O_{28}]^{6-}$, is a useful tool in deducing the interaction and the non-competitive Ca^{2+}-ATPase inhibition by the decavanadate ion $[V_{10} = V_{10}O_{28}]^{6-}$. Moreover, decavanadate and vanadate induce protein cysteine oxidation whereas no effects were detected for the decaniobate, tungstate or molybdate ions. The presence of the antioxidant quercetin prevents cysteine oxidation, but not ATPase inhibition, by vanadate or decavanadate. Definitive V(IV) EPR spectra were observed for decavanadate in the presence of sarcoplasmic reticulum Ca^{2+}-ATPase, indicating a vanadate reduction at some stage of the protein interaction. Raman spectroscopy clearly shows that the protein conformation changes that are induced by V_{10}, Nb_{10} and vanadate are different from the ones induced by molybdate and tungstate monomer ions. Here, Mo and W cause changes similar to those by phosphate, yielding changes similar to the E1P protein conformation. The putative reduction of vanadium(V) to vanadium(IV) and the non-competitive binding of the V_{10} and Nb_{10} decametalates may explain the differences in the Raman spectra compared to those seen in the presence of molybdate or tungstate. Putting it all together, we suggest that the ability of V_{10} to inhibit the Ca^{2+}-ATPase may be at least in part due to the process of vanadate reduction and associated protein cysteine oxidation. These results contribute to the understanding and application of these families of mono- and polyoxometalates as effective modulators of many biological processes, particularly those associated with calcium homeostasis.

1. Introduction

Previous studies have shown that sarcoplasmic reticulum (SR) Ca^{2+}-ATPase activity is very sensitive to the presence of several vanadium complexes such as vanadium–citrate complexes and bis(maltolato)oxovanadium(IV) (BMOV).[1,2] It has been suggested that different vanadium coordination complexes can inhibit Ca^{2+}-ATPase through specific protein–substrate interactions while the oligomeric, uncomplexed oxovanadates do not interact through the same mechanism. Moreover, the different oligovanadates such as $[VO_4]^{3-}$ (V_1), $[V_4O_{12}]^{4-}$ (V_4), or $[V_{10}O_{28}]^{6-}$ (V_{10}) may have different mechanisms and effects on the calcium ATPase activity. In particular, V_{10} is the only identified polyoxovanadate that inhibits calcium accumulation by the Ca^{2+}-ATPase when coupled to ATP hydrolysis.[3] In addition, V_{10} appears to be the most potent oxometalate Ca^{2+}-ATPase inhibitor out of all the vanadium ions and complexes so far analysed, exhibiting an IC_{50} value of 15 μM.[1–4] Recently, other transition-metal ion clusters such as niobates, tungstates and molybdates were evaluated in the inhibition of SR calcium ATPase and were found to be less efficient as inhibitors.[4] These findings were further explored, and the effects of five transition metal species, *viz.* decavanadate (V_{10}), decaniobate ($Nb_{10}O_{28}^{6-}$, Nb_{10}), vanadate (V_1), tungstate (WO_4^{3-}, W_1) and molybdate

[a]*ISE and CCmar, University of Algarve, 8005-139 Faro, Portugal*
[b]*Molecular Physical Chemistry R&D Unit, University of Coimbra, Portugal*
[c]*Department of Life Sciences, University of Coimbra, 3004-535 Coimbra, Portugal*
[d]*REQUIMTE, Centro de Química Fina e Biotecnologia, Departamento de Química, Faculdade de Ciências e Tecnologia, Universidade Nova de Lisboa, Campus da Caparica, 2829-516 Caparica, Portugal*
[e]*School of Chemistry, Monash University, Clayton, Vic 3800, Australia*
[f]*Department of Chemistry, University of California, Davis, California 95616, USA*
[g]*CCmar and FCT, University of Algarve, 8005-139 Faro, Portugal. E-mail: maalves@ualg.pt; Fax: +351 289 800066; Tel: +351 289 800905*

(MoO_4^{3-}, Mo_1) ions, on the structure and activity of SR calcium ATPase were evaluated and described in the present paper. V_{10} and Nb_{10} are isostructural and isovalent, but where vanadium is redox active and labile in solution, niobium is kinetically inert and redox stable, making Nb_{10} an excellent tool to explore the type of inhibition that the V_{10} analogue undergoes with the calcium pump. The SR calcium pump has proven to be an excellent model for studying the effects of oxovanadates and vanadium complexes on Ca^{2+} homeostasis, and by extension on several signalling processes in muscle and non-muscle cells.[1–4] Calcium homeostasis is also known to be involved in cell death processes such as necrosis and apoptosis. Finally, ion pumps are known as potential drug targets in medicine and science.[5]

Decavanadate is known to modulate the activity of many proteins such as phosphatases,[6] myosin,[7,8] and calcium pump ATPase[1–4,9,10] and to interact with proteins such as actin[11–15] among others.[16,17] Moreover, as a well-established inhibitor of tyrosine kinases and phosphatases, vanadium is suggested to be involved in the biochemical processes of several diseases, with potential uses in anticancer[18–20] and anti-diabetic therapies.[21] For instance, in rat adipocytes, the V_{10} ion has been suggested to be a more potent insulin mimetic agent than several mononuclear vanadium coordination complexes, although the precise mechanism of action is still unclear.[22] Perhaps the most notable effect of V_{10} described so far relates to the induction of mitochondrial membrane depolarization and the inhibition of oxygen consumption at nanomolar concentrations, which leads to cell necrosis.[23,24]

While the literature on the biological effects of mono- and polyoxometalates has been rapidly increasing over the most recent decade, the biochemical mechanisms underpinning the effects of these oxometalates are still only poorly understood. This is clearly a rapidly growing field, owing to the increasing interest in the use of bioavailable metal complexes in biochemistry, biology, biotechnology, pharmacology and medicine.

2. Materials and methods

All reagents were of biochemical analysis grade and were supplied by BDH, Merck, and Sigma. Anhydrous ammonium metavanadate, sodium tungstate and sodium molybdate salts were purchased from Riedel-de Haën. Tetramethylammonium decaniobate, $[N(CH_3)_4]_6[Nb_{10}O_{28}]\cdot 6H_2O$, was synthesised according to published procedures.[25,26] ATP (vanadium free) was supplied by Sigma.

2.1. Preparation of metal solutions

Decavanadate stock solution was obtained by adjusting the pH of an ammonium metavanadate solution (50 mM, pH 6.7) to 4.0, according to literature methods,[3,16,24] and the formation of the decavanadate (V_{10}) ion is readily observed by the characteristic orange colour of the solution.[16] The kinetics of decomposition of V_{10} is determined by following the absorbance at λ 400 nm of the reaction medium at 25 °C, as described elsewhere.[16,23,27] V_{10} decay follows a first-order rate law, with a half-life of more than 12 h (measured with 0.1 mM decameric vanadate species, 1 mM total vanadate), in agreement with previous work.[27] At the V_{10} concentrations and time-scales used in the enzymatic studies performed in the present work, the vanadium solution contains almost exclusively the decameric species. On the other hand, vanadate solutions up to 1 mM contain mostly monomeric, dimeric and tetrameric vanadate species, as determined using NMR spectroscopy.[3,27] Stock solutions of sodium tungstate and sodium molybdate were prepared in milliQ water. A solution of decaniobate was prepared in water as a stock concentration of 10 mM, with a self-buffered pH of 6.0. Decaniobate solutions are stable under these conditions, as shown elsewhere.[25,26] Under the experimental conditions used in this study, the addition of the metals to the reaction medium, within the concentration ranges used in the study, did not change the pH of the medium.

2.2 Preparation of sarcoplasmic reticulum vesicles

Isolated sarcoplasmic reticulum vesicles (SRV), prepared from skeletal rabbit muscles, were suspended in 0.1 M KCl, 10 mM HEPES (pH 7.0), diluted 1 : 1 with 2.0 M sucrose and frozen in liquid nitrogen prior to storage at −80 °C, as described elsewhere.[3,11] The protein concentration was determined spectrophotometrically at 595 nm, by the Bradford method, using bovine serum albumin as a standard and in the presence of 0.125% of sodium dodecyl sulphate (SDS). The percentage of each protein present in the SR-vesicle preparations was determined through densitometry analysis of SDS-polyacrylamide gel electrophoresis (7.5% acrylamide). The SR Ca^{2+}-ATPase analysed by SDS polyacrylamide gel electrophoresis comprised at least 70% of the total protein in the SR-vesicles. The SERCA-1 (sarcoplasmic, or endoplasmic reticulum Ca^{2+}-ATPase-1) was the predominant isoform in our SR preparations.[28]

2.3 ATP hydrolysis by a calcium pump

Steady-state assays of the sarcoplasmic reticulum Ca^{2+}-ATPase were measured spectrophotometrically at 25 °C using the coupled enzyme pyruvate kinase/lactate dehydrogenase assay, as described elsewhere,[2,28] under the following conditions: 25 mM HEPES (pH 7.0), 100 mM KCl, 5 mM $MgCl_2$, 50 μM $CaCl_2$, 2.5 mM ATP, 0.42 mM phosphoenolpyruvate, 0.25 mM NADH, 18 IU lactate dehydrogenase and 7.5 IU pyruvate kinase, with or without vanadate, decavanadate, decaniobate, tungstate or molybdate, in the absence or in the presence of the following antioxidants, wherever stated: glutathione (GSH) (1 mM), quercetin (10 μM) or kaempferol (10 μM). The experiments were initiated by the addition of 10 μg mL^{-1} calcium ATPase, in the presence or absence of 4% (w/w) of calcium ionophore A23187, and followed for 5 min. Metal solutions were added to the medium immediately prior to protein addition. The absorbance of the metal solutions did not interfere with the determination of the reaction rates at the chosen wavelength of 340 nm. Furthermore, within the concentration range studied, the oxometalates did not affect the coupled enzyme method used in the assays, as observed upon addition of 40 μM ADP.

2.4 Measurements of reduced cysteine residues

The titration of accessible reduced cysteine residues in sarcoplasmic reticulum Ca^{2+}-ATPase was done in the absence of denaturants and was performed with DTNB (5,5′-dithiobis-(2-nitrobenzoic acid)), as indicated in previous work,[13,23,24,29] using an extinction coefficient at 412 nm of 14.150 M^{-1} cm^{-1} for the colored product TNB (2-nitro-5-thiobenzoate). The assays were carried out in HEPES (pH 7.0), 100 mM KCl, 5 mM $MgCl_2$ and 55 mM sodium-phosphate buffer (pH 7.2), following 5 min of incubation of 0.2 mL SR (1 mg mL^{-1}) with vanadate, decavanadate, decaniobate, tungstate or molybdate, in the absence or in the presence of the following antioxidants, wherever stated: quercetin (10 or 100 μM) or kaempferol (10 or 100 μM).

2.5 Electron paramagnetic resonance spectroscopy

X-band (9.65 GHz) EPR spectra were acquired on a Bruker EMX 6/1 spectrometer equipped with a Bruker ER4116DM rectangular cavity. The samples were cooled to 77 K with an Oxford Instruments ESR900 continuous-flow cryostat (with liquid helium), fitted with a temperature controller. The acquisition conditions involved a field modulation frequency of 100 kHz, a 10 G modulation amplitude, a microwave power of 635 μW, a time constant of 163.840 ms, with a sweep time of 335.544 s; the spectra were acquired by sweeping the magnetic field between 2400 and 4400 G. The decavanadate reduction and subsequent vanadyl(IV) formation were evaluated using the same samples prepared for the NMR measurements (*vide infra*).

2.6 NMR measurements

^{51}V NMR spectroscopy measurements were performed on a Bruker AM-400 MHz (9.4 T; ^{51}V 105.2 MHz) spectrometer equipped with a 5 mm multinuclear inverse probe. Spectra were acquired at 22 °C using 0.5 mL of samples containing 10% D_2O using a calibrated π/2 pulse. 12 000–25 000 scans were acquired with recycling delays of 10 ms, acquisition times of 86 ms at a spectral width of 45.454 kHz, as described elsewhere.[3]

The ^{51}V-NMR chemical shifts are reported relative to an external reference of $VOCl_3$, as described in previous work.[1–4,27] NMR spectra of decavanadate (5 mM total vanadium) in a reaction medium containing 25 mM HEPES (pH 7.0), 100 mM KCl, 5 mM $MgCl_2$ and 50 μM $CaCl_2$ were obtained in the absence or in the presence of sarcoplasmic reticulum vesicles (5 mg mL^{-1} total protein) and 2.5 mM ATP. Similarly, NMR spectra were obtained in the presence of 1 mM of decaniobate (Nb_{10}) in the absence or presence of 2.5 mM ATP. The reported ^{51}V-NMR line widths of the free and bound vanadate resonances represent the full widths at half-maximum ($\Delta\nu_{1/2}$) height after subtraction of the 20 Hz used for exponential line broadening during processing. The concentration of each vanadate species V_x was calculated from the fractions of the total integrated areas using the following equation: $[V_x] = (A_x/A_t) \times ([V_t]/n)$, where A_x corresponds to the area measured for the vanadate species X with n aggregation number (number of vanadium atoms), A_t the sum of measured areas, and $[V_t]$ the total vanadate concentration, as described elsewhere.[3,23,27]

2.7 Atomic absorption analysis

Vanadium analysis was performed by atomic absorption spectroscopy (AAS), as described elsewhere.[4] Briefly, all the protein samples in a reaction medium similar to the above NMR studies, in the absence and in the presence of decavanadate, were centrifuged at 17 000 rpm (40 000*g*), during 60 min at 4 °C. The supernatant solutions over the centrifuged samples were then analysed using a GBC Avanta atomic absorption spectrometer.[4] The vanadium lamp was operated at 318.2 nm, with a slit width of 0.2 nm, and the instrument was calibrated against a series of solutions containing 50, 100, 150 and 200 ppb of vanadium. Calibration standards were obtained by successive dilutions of a Merck standard solution of vanadium 1002 ± 2 mg L^{-1}. The detection and quantification limits of the instrument for these analysis conditions, determined according to ISO 8466-1, were 5 ± 1 μg L^{-1} of vanadium. The method was validated using a certified reference material (TORT-1's vanadium content 1.4 ± 0.3 mg kg^{-1}) purchased from the National Research Council of Canada.

2.8 Raman spectroscopy

The Raman spectra were obtained at room temperature, in a triple monochromator Jobin-Yvon T64000 Raman system (focal distance 0.640 m, aperture f/7.5) equipped with holographic gratings of 1800 grooves per mm. The premonochromator stage was used in the subtractive mode. The detection system was a liquid nitrogen cooled non-intensified 1024 × 256 pixel (1″) Charge Coupled Device (CCD) chip. The 514.5 nm line of an Ar^+ laser (Coherent, model Innova 300-05) was used as the excitation radiation, providing *ca.* 50 mW at the sample position. A 90° geometry between the incident radiation and the collecting system was employed. The entrance slit was set to 200 μm, and the slit between the premonochromator and the spectrograph was 400 μm.

Samples were sealed in Kimax glass capillary tubes of 0.8 mm inner diameter. Under the above mentioned conditions, the error in wavenumbers was estimated to be within 1 cm^{-1}.

2.9 Statistical analyses

All parameters studied are present as averages and standard deviations of measurements taken from triplicate measurements from three SR preparations. Student's *t*-test pairwise sets were used.

3. Results and discussion

Oxometalates, in particular decavanadate (V_{10}), can act as dramatic inhibitors (IC_{50} = 15 μM) of the hydrolytic activity of sarcoplasmic reticulum Ca^{2+}-ATPase,[1] a transmembrane protein involved in calcium translocation and responsible for muscle relaxation.[30] Vanadium is used as a functional and structural tool in many biological studies involving ion pumps and other types of enzymes, since it is well established that monomeric vanadate(V) can mimic transition states involved in phosphoryl-transfer reactions, once the chemical structure is very similar to phosphate.[31] However, the physiological role of vanadium and the mode of

action in the hydrolytic activity of sarcoplasmic reticulum Ca^{2+}-ATPase, an important process in Ca^{2+} homeostasis, are not understood. In the present study, we further investigate the effects of niobate, vanadate, molybdate and tungstate oxometalates on the structure and function of the sarcoplasmic reticulum Ca^{2+}-ATPase, in order to reveal new insight into metal–protein interaction processes and the effects on calcium homeostasis, by combining NMR, atomic absorption, EPR and Raman spectroscopies with enzyme kinetic studies.

3.1. NMR and enzymatic studies

Early work using ^{51}V-NMR to explore the interaction between oxovanadates and proteins focussed on SR Ca^{2+}-ATPase,[9] but since then the method has been applied to a variety of biomolecules including the muscle proteins myosin and actin, among others.[3,12,16,17,32–35] In general, it was found that the interaction of the protein with a specific vanadate(v) species induced changes in the intensity and shape of the correspondent vanadate NMR signals. In some studies, these changes were not observed if the interaction was prevented by the presence of the protein's natural ligands,[3,12,33] offering an insight into the preferred modes of interaction of vanadium with these substrates. In the present study, broadening of the observed V_{10} NMR signal showed that V_{10} interacts with the calcium pump, the interaction being stronger in the presence of ATP, the natural ligand of SR ATPase, once the $\Delta\nu_{1/2}$ increased from 3 to 4 (Fig. 1A, Table 1). V_{10} typically shows a 1 : 2 : 2 ratio of 3 peaks, namely 10A, 10B and 10C, in its ^{51}V NMR spectrum (Fig. 1A).[3,12,33,34] Similar line broadening has been described in cases where oligomeric oxovanadates were associating with a protein[3,11,12,16,33] or with a lipid structure.[34] Moreover, it was observed that Nb_{10} prevents the interaction of the isostructural V_{10} with the protein, as evidenced by a sharpening of the decavanadate signal once the V_{10A} line broadening decreases from 3 to 2.5 (Fig. 1B, Table 1), suggesting that they compete for the same binding site, a site which is different from the ATP binding site. C_2 and C_1 are NMR signals ascribed to vanadate–sucrose complexes, described elsewhere,[3] once the SR Ca^{2+}-ATPase samples contain sucrose.

Although V_{10} has been shown to be an enzyme modulator,[4,6,16,17,35] little is known about the type of inhibition it engages in.[3,4,6] In addition, the rich solution chemistry of vanadium as evidenced by its propensity to form a wide range of species in solution coupled with the thermodynamic lability of the V_{10} ion specifically opens up the possibility that the species of vanadium present in solution under the experimental conditions may not always be the one intended – or even suspected. This is particularly true for experiments that require long incubation times, complex solvent compositions or elevated temperatures, which increases the rates of V_{10} decomposition.[16,17,23,24,27,35] Because of this it is imperative that the vanadium species present in solution are carefully characterised before attributing a particular biological effect or a biochemical mechanism to a specific ion species.[3,16,17,23,24,27,35]

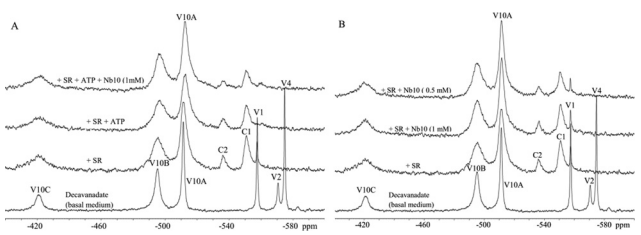

Fig. 1 105.2 MHz ^{51}V-NMR spectra, at room temperature, of 0.5 mM decavanadate (5 mM total vanadate) in 25 mM HEPES (pH 7.0), 100 mM KCl, 5 mM $MgCl_2$, 50 μM $CaCl_2$ with (A) SR calcium ATPase, plus 0.25 mM ATP or niobate, and (B) upon niobate addition.

In the present study, the inhibition of the ATPase activity by V_{10} was found to be competitive for lower concentrations (10 μM) and non-competitive for higher concentrations (50 μM) (Fig. 2A) of V_{10}. Previously, it was shown that the isostructural Nb_{10} inhibits non-competitively at both concentrations.[4] However, while Nb_{10} is stable and relatively inert under these conditions, V_{10} is not and is highly reactive. The formation and presence of monomeric vanadate might be responsible for the processes of competitive inhibition, seen at lower V_{10} concentrations (10 μM). Therefore, it is suggested that while V_{10}, like Nb_{10},[4] interacts with calcium ATPase non-competitively, the formation of monomeric vanadium(v) species is responsible for competitive interaction. This is similar to what is seen for tungstate (Fig. 2B). Tungstate (W_1) has a lower SR Ca^{2+}-ATPase inhibition capacity than decavanadate[4] (IC_{50} = 400 μM for W_1 and IC_{50} = 15 μM for V_{10}), although higher than described for Na^+-K^+-ATPase inhibition (W_1 IC_{50} = 1.5 mM).[36] For this enzyme, other polyoxotungstates (W_{12}) present a higher capacity of inhibition, with IC_{50} less than 15 μM, the value found above for V_{10}.[36] It thus seems that the decavanadate–calcium pump interaction is favoured in the presence of ATP but is prevented by the iso-structural and iso-electronic decaniobate ion and V_{10} non-competitively inhibits the enzyme activity *vis-à-vis* ATP. Other studies, however, have found that the interaction of V_{10} with the calcium pump is competitive, it binds to two sites,[9,37] and have suggested that V_{10} will bind to the calcium pump at the vanadate-binding site, or to the nucleotide binding site.[9,37,38] This has led to the suggestion that the V_{10}-binding site is the same as the ATP binding site or at least close to it, since it has been observed that a covalent inhibitor that binds specifically to Lys-515 within the ATP binding site also prevents V_{10} from binding to the ATPase.[38]

Structural studies based on V_{10}-induced crystallization of the calcium pump complex have indicated that the V_{10} binding site in the E2 conformation of the SR ATPase is located in the intersection of the three cytoplasmic protein domains that includes the nucleotide, the phosphorylation and the β-strand domains.[10] It should be noticed that some ATPase enzymes include many membrane enzymes such as the E1E2-ATPases. Although many details are known with regard to the biochemical mechanisms of these ATPases, inhibitory studies assume that vanadate acts as a phosphate analogue and presumably inhibits the enzymes as a transition-state analogue for the phosphoryl group transfer. However, E1–E2 ATPases are not truly an ATPase but a phosphohydrolase, once what is hydrolyzed is the phosphate that is covalently bound to the enzyme, rather than ATP. Further studies are needed to clarify the interaction and the effects of V_{10} on the structure and function of the calcium pump, once it seems that it does not behave like vanadate, a phosphate analogue.

Table 1 Chemical shifts (δ), line widths ($\Delta\nu_{1/2}$), and broadening factor of the line widths (f) of monomeric (V_1), dimeric (V_2), tetrameric (V_4) and decameric (V_{10}) forms of vanadate present in 5 mM nominal decavanadate solution (0.5 mM V_{10}) under different experimental conditions

Decavanadate (0.5 mM)								
	V_{10C}	V_{10B}	V_{10A}	V_1	V_2	V_4	C_2	C_1
Medium								
δ/ppm	−421.0	−495.0	−512.0	−558.0	−571.0	−575.0	−537.0	−551.0
$\Delta\nu_{1/2}$/Hz	1394.0	996.0	398.0	199.0	398.0	199.0		
Area	2.5	6.4	10.4	4.3	1.0	5.6		
[+SR Ca^{2+}-ATPase (5 mg mL^{-1})]								
δ/ppm	−421.0	−495.0	−512.0	−558.0	−571.0	−575.0	−537.0	−551.0
$\Delta\nu_{1/2}$/Hz	2788.0	2390.0	1195.0	199.0			996.0	1095.0
f	**(2.0)**	**(2.4)**	**(3.0)**	**(1.0)**				
Area	3.6	5.4	8.5	1.2			1.0	2.8
[+SR Ca^{2+}-ATPase (5 mg mL^{-1}) + ATP (2.5 mM)]								
δ/ppm	−421.0	−495.0	−512.0	−558.0	−571.0	−575.0	−537.0	−551.0
$\Delta\nu_{1/2}$/Hz	3386.0	2589.0	1593.0				1195.0	1195.0
f	**(2.4)**	**(2.6)**	**(4.0)**					
Area	2.9	5.4	6.9				0.9	2.0
[+SR Ca^{2+}-ATPase (5 mg mL^{-1}) + Nb_{10} (1 mM)]								
δ/ppm	−421.0	−495.0	−512.0	−558.0	−571.0	−575.0	−537.0	−551.0
$\Delta\nu_{1/2}$/Hz	2190.0	1991.0	996.0	199.0			996.0	1095.0
f	**(1.6)**	**(2.0)**	**(2.5)**	**(1.0)**				
Area	2.6	5.8	9.6	0.9			0.8	2.0
[+SR Ca^{2+}-ATPase (5 mg mL^{-1}) + Nb_{10} (0.5 mM)]								
δ/ppm	−421.0	−495.0	−512.0	−558.0	−571.0	−575.0	−537.0	−551.0
$\Delta\nu_{1/2}$/Hz	2788.0	2190.0	996.0	199.0			1195.0	1195.0
f	**(2.0)**	**(2.2)**	**(2.5)**	**(1.0)**				
Area	3.3	5.8	9.5	0.6			0.8	2.0
[+SR Ca^{2+}-ATPase (5 mg mL^{-1}) + ATP (2.5 mM) + Nb_{10} (1 mM)]								
δ/ppm	−421.0	−495.0	−512.0	−558.0	−571.0	−575.0	−537.0	−551.0
$\Delta\nu_{1/2}$/Hz	2788.0	1991.0	1195.0				1195.0	1195.0
f	**(2.0)**	**(2.0)**	**(3.0)**					
Area	2.9	4.7	8.4				0.5	1.4

3.2. Atomic absorption and EPR spectroscopy with cysteine oxidation studies

Using atomic-absorption spectroscopy (AAS) V_{10} has been shown to bind to an equal extent to all protein conformations that occur during the process of calcium translocation, *viz.* E1, E1P, E2 and E2P.[4] Thus the amount of V_{10} that was found to bind to each conformer of the enzyme was the same, and was independent of the medium conditions that favoured each protein conformation. A likely possibility is that the V_{10} binding is always available independently of the calcium translocation-dependent conformational changes. This is in stark contrast with what has been observed for monomeric vanadate, as vanadium binding to the protein is clearly prevented in the E1 conformation, but is favourable when the protein is in the E2 conformation.[4,10]

In this study we observe that Nb_{10} prevents the interaction of V_{10} with the calcium pump once the amount of vanadium bound to the protein decreases by about 50%, whereas no effects were observed for heparin, a molecule known to interact with nucleotide binding sites (Fig. 3). Using NMR it was confirmed that the isostructural Nb_{10} prevents the V_{10} from interacting with the protein. The fact that V_{10} inhibition would be non-competitive, as suggested above, and that the interaction with the calcium pump is independent of the protein conformation may point to a specific mode of interaction with the calcium pump that is clearly different from the one described for vanadate alone. This observation, in agreement with previous functional studies executed at conditions very close to physiological ones, means that V_{10} is the only vanadate species able to prevent calcium translocation coupled to ATP hydrolysis, whereas no effect is found for a normal vanadate solution, not containing V_{10}, up to concentrations of 2 mM.[3]

On the other hand, more recently the IC_{50} value of calcium ATPase inhibition for Nb_{10} (IC_{50} = 35 μM) was found to be more than twice that of V_{10} (IC_{50} = 15 μM).[4] This shows that V_{10} may have a different mode of protein interaction. Monomeric vanadate (V_1), a product of V_{10} decomposition in the medium, may also contribute to the inhibition effects. However, as indicated by AAS, monomeric vanadate interaction should not be favoured under conditions where calcium is present and the E1 conformation is dominant. In addition, the inhibition of the calcium ATPase by monomeric vanadate is less effective. There is evidence that vanadate can form a complex with ATP itself, as is expressed through broadening of the monomeric vanadate signal in the presence of ATP,[3] and a similar type of complex formation has been suggested with myosin.[11,12] It is also possible that the V_{10} mediated inhibition of calcium ATPase

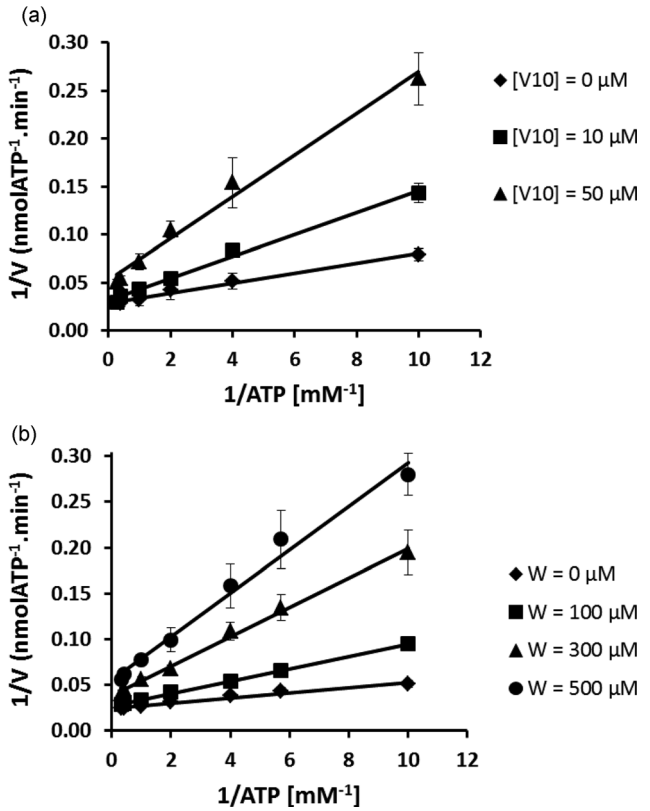

Fig. 2 (A) Lineweaver–Burk plot of the inhibition of the sarcoplasmic reticulum calcium pump with V_{10}. Concentrations in vanadium are referred as decavanadate concentrations. ATPase activity was measured as indicated in the Materials and methods section. Data are plotted as means ± SD. The results shown are the average of triplicate experiments. (B) Lineweaver–Burk plot of the inhibition of the sarcoplasmic reticulum calcium pump with W. Concentrations in tungstenium are referred as tungstate concentrations. The ATPase activity was measured as indicated in the Materials and methods section. Data are plotted as means ± SD. The results shown are the average of triplicate experiments.

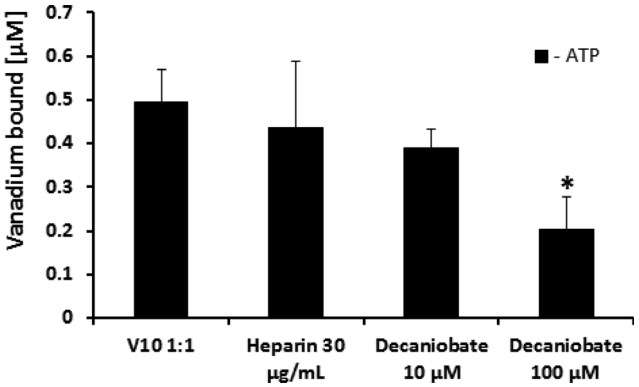

Fig. 3 Vanadium analysis performed by atomic absorption spectroscopy (AAS). V_{10} samples containing 1 μM vanadate species, upon addition of an equal concentration of sarcoplasmic reticulum (SR) calcium ATPase (1 μM), in the presence of heparin or decaniobate, in the medium containing 25 mM HEPES (pH 7.0), 100 mM KCl, 5 mM $MgCl_2$, 50 μM $CaCl_2$ and 0.25 mM ATP, were centrifuged and the supernatant analyzed by AAS, as described in the Materials and methods section. The concentrations of vanadium, for V_{10} solutions, were plotted against the several medium conditions. Data are plotted as means ± SD. The results shown are the average of triplicate experiments.

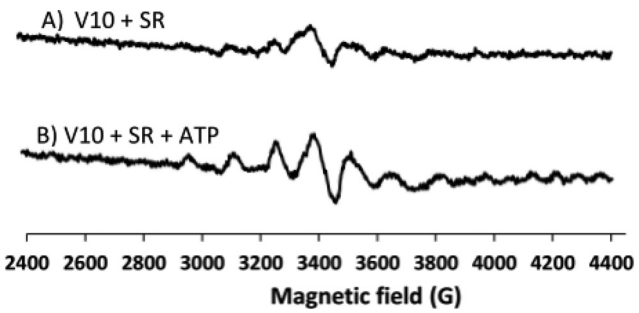

Fig. 4 X-band EPR spectra of 0.5 mM decavanadate (5 mM total vanadate) in 25 mM HEPES (pH 7.0), 100 mM KCl, 5 mM $MgCl_2$, 50 μM $CaCl_2$ with SR calcium ATPase, in the absence (A) and in the presence of 0.25 mM ATP (B). The spectra were acquired as described under Materials and methods. Upon protein addition the oxidovanadium(IV) typical signals are elicited.

involves oxidation of the cysteine units in the protein, which would certainly affect the activity of the enzyme.[39] This would also lead to the reduction of vanadate(V) to vanadyl(IV), which is an EPR active species. Such a signal was indeed found, and only for either vanadate or V_{10} incubation with calcium ATPase (Fig. 4), but not in the absence of the calcium ATPase. This is strong evidence that cysteine units in the protein are oxidized in the presence of vanadium(V), as has previously been reported in similar experiments with myosin or with actin.[12,13,40]

Actin was described as a potential target for decavanadate, being suggested to reduce the metal and to bind with vanadyl with a 1.1 stoichiometry.[11–15] This explains the difference in the inhibition caused by Nb_{10} *vs.* V_{10} in spite of them being isostructural and isovalent: while the standard reduction potential of VO_2^+ to VO^{2+} is +1.0 V, under acidic conditions niobium(V) isn't known to be easily reduced.[25,26] This difference in redox activity means that while vanadate can reduce cysteine ($E_0 \sim -0.15$ V, values referred are *vs.* the standard hydrogen electrode and reported at pH 7), niobate won't. In fact, only the vanadate and V_{10} species induced protein cysteine oxidation, whereas no evidence of oxidation was detected for the other Nb, W and Mo oxometalates (Fig. 5). Furthermore, adding antioxidants such as quercetin or kaempferol (100 μM) partially reversed the cysteine oxidation induced by vanadate (Fig. 5). With other antioxidants, such as GSH (1 mM), it was not possible to evaluate the effect, due to interferences in the method, because the compounds absorbed at the wavelength of the measurement or it formed complexes with the antioxidants. For the same reasons the antioxidant reversion of cysteine oxidation induced by V_{10} could not be determined. Apparently, V_{10} is reacting with the antioxidant. All the data, however, point towards the oxidation of cysteine being a key part of the inhibitory mechanism of V_{10} towards calcium ATPase. On the other hand, it means that vanadate can be reduced by thiols not only in biological conditions,[41] but particularly upon interaction with specific proteins such as actin[13] and also with the calcium pump, as described above.

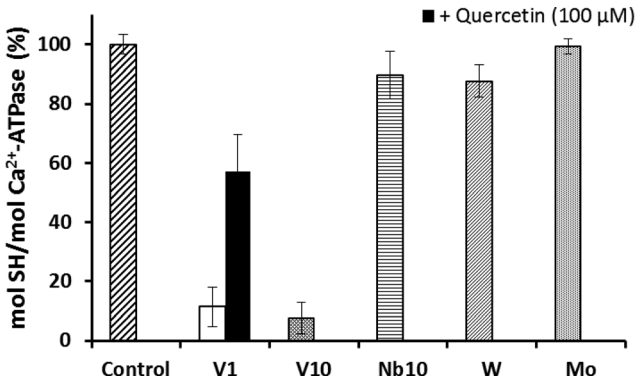

Fig. 5 Calcium ATPase cysteine (Cys) redox state, after oxometalates exposition. The accessible thiol groups, in the absence of denaturants, were measured as indicated in the Materials and methods section. Data are plotted as means ± SD. The results shown are the average of triplicate experiments. Titration of cysteines was carried out in HEPES (pH 7.0), 100 mM KCl, 5 mM $MgCl_2$ and 55 mM sodium phosphate buffer (pH 7.2), after 5 min of incubation of 0.2 mL SR (1 mg mL^{-1}) with vanadate (1 mM), decavanadate (0.3 mM), decaniobate (0.035 mM), tungstate (8 mM) or molybdate (45 mM), in the absence or in the presence of the following antioxidants, wherever stated: GSH (1 mM), quercetin (100 µM) or kaempferol (100 µM). The increase in absorbance at 412 nm was continuously recorded over 5 min, until a steady value was reached. The results shown are the average of triplicate experiments.

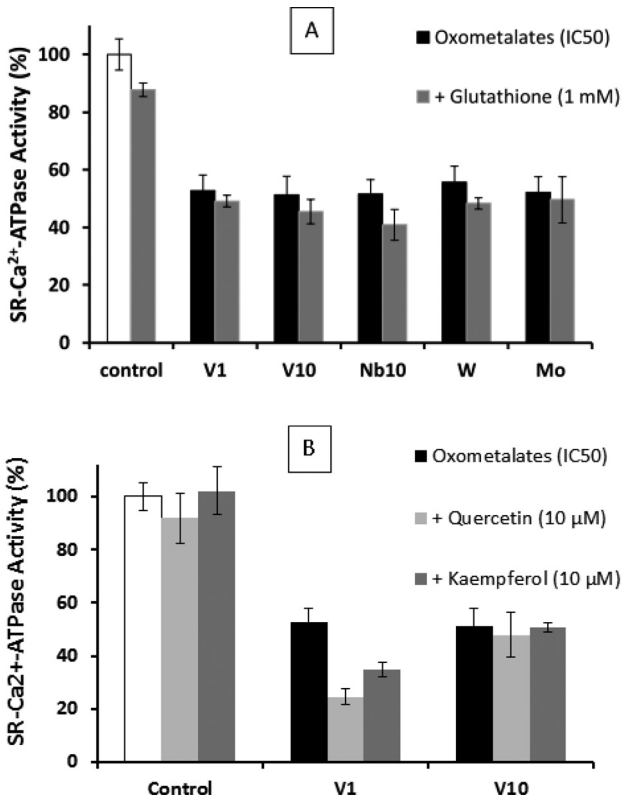

Fig. 6 Effect of reduced glutathione (GSH) on sarcoplasmic reticulum (SR) Ca^{2+}-ATPase activity in the presence of oxometalates, at IC_{50} concentrations. The ATPase activity was measured as indicated in the Materials and methods section. Data are plotted as means ± SD. The results shown are the average of triplicate experiments.

It has been suggested that only one or two cysteine (Cys) residues of the SR Ca^{2+}-ATPase are critically important for the function of the enzyme.[39] Modification of Cys349, located near the phosphorylation binding site, causes modulation of the SR Ca^{2+}-ATPase activity by peroxynitrite.[42] In this case the oxidation could be reverted by GSH, but for high concentrations of oxidizing agents the content of the SH group decreases and the effect cannot be reverted, *i.e.* the oxidation is irreversible.[39] In fact, Ca^{2+}-ATPase inhibitory effects promoted by reactive oxygen and nitrogen species,[39,42] as well as the antitumor drug 3-bromopyruvate,[43] all appear to involve protein cysteine oxidation. To verify that glutathione (GSH) could reverse the decrease in calcium ATPase activity induced by the oxometalates, GSH was added to the medium just prior to oxometalate addition. Although cysteine oxidation was still observed for the two vanadate solutions, GSH could not prevent or revert the inhibition and similar IC_{50} values were obtained with or without GSH (Fig. 6A), for all the oxometalates. Quercetin and kaempferol, antioxidants present in tea, grapes and apples, were also ineffective, suggesting that the inhibitory effects are not a consequence of cysteine oxidation, or that the specific cysteine oxidation does not contribute significantly for the modulation of the ATPase activity (Fig. 6B).

Therefore it is suggested that V_{10} induces oxidation of cysteine but that only partially modulates the ATPase activity. Speculating, this cysteine unit is likely located near the nucleotide binding site, such as Cys675 or Cys674, not particularly involved in the modulation of the enzyme activity. Decavanadate binding to the calcium ATPase may involve all the three cytoplasmic domains, but near the phosphorylation binding site, as described elsewhere.[10,44] Decavanadate fits in the protein like a ball in a vise preventing the vise from closing.[44] This binding locus would explain the inhibitory effect V_{10} has on SR Ca^{2+}-ATPase activity and on calcium translocation, as described previously.[3,4,16,17,35]

3.3. Raman spectroscopy studies

In order to better understand the structural changes induced by the oxometalates on the calcium ATPase, the process was studied using Raman spectroscopy to explore the conformations of calcium ATPase which dominate in the presence of oxometalates. Raman spectroscopy is highly sensitive towards small structural changes in protein structure and has been a versatile tool in investigating protein structure modification caused by metal interactions.[45,46]

As is the case with infrared spectroscopy, the Raman spectrum contains several diagnostic regions which correspond to specific vibrational modes belonging to common structural motifs seen in proteins.[45–48,50–52] These include a band at *ca.* 855 cm^{-1} which belongs to tyrosine residues, and a band at *ca.* 930 cm^{-1} indicative of α-helices[46–48,50] (Fig. 7A). Raman spectroscopy has been used to follow peptide tyrosine phosphorylation using the two bands between 820 and 855 cm^{-1} [48–50] that are observed in the absence of phosphorylation.

Several bands that are sensitive to the average conformation of the protein can be identified in the Raman spectrum, and these can be used to evaluate the protein conformational changes

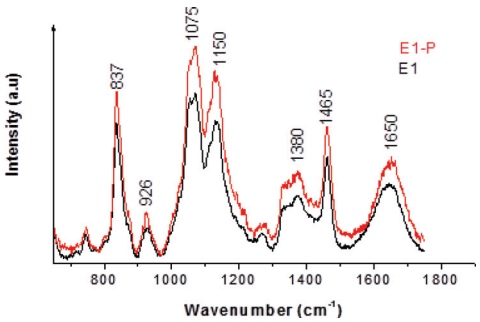

Fig. 7 Raman spectra of calcium ATPase at conformation states E1 upon phosphorylation (E1P).

induced by external or internal factors. For instance, peptide tyrosine phosphorylation results in two bands at *ca.* 825 and 853 cm^{-1}.[48–50] The ratio of intensities of these bands gives indications about the strength of tyrosine hydrogen bonding.[48–50] In the present study, this Fermi resonance doublet was not observed, but instead only a single band at 837 cm^{-1} (Fig. 7A) was found. Such an observation could be interpreted in two ways: (i) the tyrosine units are not involved in hydrogen bonding[48] or (ii) the tyrosine residues are phosphorylated, leading to the collapse of the doublet into a single band.[48–50] While the first hypothesis should be discarded, because the tyrosines would have to be facing the interior of the protein instead of interacting with bulk water, the second one is unlikely because it is known that the Ca^{2+}-ATPase is phosphorylated in aspartic acid.[30,32]

In the present study, we collected spectra on protein conformation E1 – medium containing calcium, or on protein conformation E1P, in the presence of ATP (Fig. 7A). It is suggested that the more intense peak at 1650 cm^{-1} corresponds to the amide I C═O stretching vibration of the peptide, and the peak at 1150 cm^{-1} probably can be assigned to the CH_2 deformation from lipid hydrocarbon,[51,52] once the sample contains not only the membranar protein but also the native lipid bilayer from the sarcoplasmic reticulum. The changes in the intensity of the peak at 1150 cm^{-1} can be probably due to metal-induced changes to the CH_2 in lipid molecules,[52] that would suggest an effect on the lipid-membrane structure. An increase in the peak at 1650 cm^{-1}, ascribed to amide I (C═O stretching vibration of the peptide), is also observed (Fig. 7A), indicating changes in the secondary structure of the protein. No significant changes were detected, when the protein is susceptible to phosphorylation by inorganic phosphate, in a medium containing EGTA that complexes all the free calcium and inorganic phosphate (not shown). These conditions favour conformation E2 and by extension the E2P conformation. Also by comparing the Raman spectra of the calcium ATPase in both conformations E1 and E2, no significant differences were detected (not shown), in agreement with observations in similar studies with the Na^+, K^+, ATPase.[52]

Both molybdate and tungstate induce distinct changes in the intensities of the peaks (Fig. 8A and B), suggesting that those oxometalates are promoting different protein conformation changes. In comparison with the E1P spectra, upon addition of Mo, peaks at 837, 1075 and 1465 cm^{-1} did not change, while the peak at 1650 cm^{-1} is more intense and peaks at 926, 1150

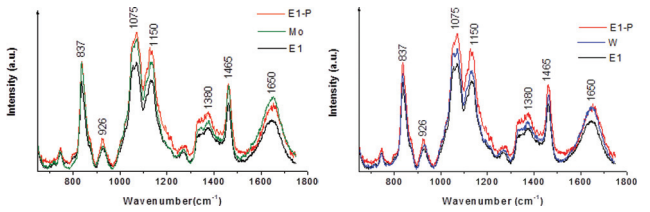

Fig. 8 Raman spectra of calcium ATPase in the presence of molybdate (left) or tungstate (right) in the medium. Mo decreases the peak at 1150 cm^{-1}, and it increases the peak at 1650 cm^{-1}, belonging probably to the CH_2 deformations in lipid molecules and the amide I C═O stretching vibration of the peptide, respectively. For W, a decrease in the bands, in comparison with E1P, was detected for all the first six peaks, whereas the last peak at 1650 cm^{-1}, shows the same intensity.

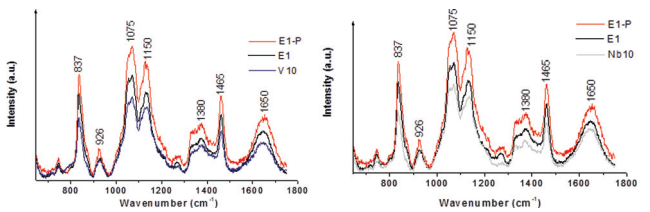

Fig. 9 Raman spectra of calcium ATPase upon addition of decavanadate (left) or decaniobate (right).

and 1380 cm^{-1} are weaker (Fig. 8A). For W, a decrease in the bands, relative to E1P, was detected for all the first six peaks found in the spectra whereas the last peak at 1650 cm^{-1} remained unchanged (Fig. 8B). For Mo, the increases on α-helices point to a structure-organizing effect, but clearly the Mo interaction seems to induce different calcium ATPase protein conformational changes than W, although as described above they both favour an E1 type conformation. In contrast to the former oxometalates, upon incubation of the protein with Nb_{10} or V_{10}, a decrease in the intensities of all the peaks was observed (Fig. 9). Furthermore, the decrease in the intensities of all the peaks upon V_{10} and Nb_{10} interaction, observed for the E1 conformation, was also detected in the Raman spectra of the enzyme in the E2 conformation, that is, absence of free calcium due to the presence of EGTA in the medium, suggesting that those oxometalates affect both spectra of the E1 or E2 protein conformation (not shown).

In contrast to the effects induced by V and Nb on the protein Raman spectra at the E1 or E2 conformation, no significant changes were detected in the Raman spectra upon phosphate or tungstate addition to the enzyme in the E2 conformation, whereas a small decrease was observed for molybdate (not shown). Note that the presence of any natural ligand of the Ca^{2+}-ATPase will induce major conformational changes in the protein, thus affecting oxometalate interactions. In addition to the binding to the cytoplasmic domains, other binding sites for decameric vanadate have been suggested, such as the specific intermolecular binding sites described to be essential to induce crystal formation.[9,10] Therefore, although it has been used to resolve the structure of enzyme in the E2 state,[10] V_{10} seems to behave unlike a natural ligand of the enzyme.

Raman spectroscopy can also be used to characterize oxometalate solutions,[53] the exploration of the viability of this approach

to decavanadate and decaniobate solutions is currently underway. A preliminary study suggests that the more stable Nb_{10} oxometalate is an excellent tool to elucidate V_{10} chemistry in solution (Batista de Carvalho *et al*., unpublished results). Based on the data, it appears that V_{10} and Nb_{10} induce similar Ca^{2+}-ATPase conformational changes, which are different from the known conformers E1 or E2, once similar changes in the Raman spectra were detected (Fig. 9 and not shown). W and Mo cause yet another set of conformations. It is suggested that tungstate and molybdate induce the same type of structural changes that are seen in inorganic phosphorylation, but that Nb_{10}, vanadate and V_{10} cause different changes corresponding to an as of yet unknown type of structure. These latter oxometalates interact with both the E1 and E2 states, while this is not the case of the tungstate and molybdate. It is clear that Raman spectroscopy can be a useful diagnostic tool in providing additional information on the effect of oxometalates on calcium ATPase conformation and as such complements EPR and NMR.

4. Conclusion

In spite of the attention paid to the role of oxometalates in biological systems in recent years, their potential and modes of action are still poorly understood. For example, their influence on the activity of calcium pump ATPase, a key enzyme in homeostasis, is yet to be fully understood. Based on the findings in this study, it is concluded that V_{10} shows a specific interaction with the calcium pump in comparison to other oxometalates. It induces cysteine oxidation and undergoes non-competitive inhibition. The ATPase inhibition is not reverted by GSH or quercetin, but the cysteine oxidation is partially prevented by antioxidants such as quercetin. Moreover, V_{10} does not discriminate against any of the protein conformations that occur during the process of calcium translocation, but binds to all of them. Raman spectroscopy points to specific calcium ATPase conformational changes being induced by the oxometalates, but that these changes depend on what oxometalates are present. Therefore, this work confirms the fact that vanadate interaction with proteins, not only with actin but also with SR Ca-ATPase, can impact thiols and undergoing vanadium reduction. It is believed that the present observations will contribute to the understanding of oxometalate interactions with the calcium pump and the role of V_{10} in biology, particularly the mechanisms of V_{10} interaction with ionic pumps.

The isostructural Nb_{10} is shown to be an excellent tool for clarifying the mode of interaction and the effects of V_{10} on the calcium pump. Raman spectroscopy points to a new approach on the interaction of oxometalates with the calcium pump, finding distinct protein conformational changes, similar to E1P or to none of the established conformations induced by the presence of oxometalates. Putting it all together, it is suggested to be due to the putative reduction of vanadate as well as the non-competitive V_{10} binding, and would explain why monomeric molybdate and tungstate behave differently regarding the interaction with the SR calcium pump. We conclude that it is the V_{10} or the vanadate interaction with calcium ATPase which induces cysteine oxidation and the concomitant vanadate reduction. Therefore, many aspects of the interactions between the different oxometalates and the calcium pump are yet to be clarified. Although some are chemically very similar they induce different effects on the structure and on the function of the protein.

Abbreviations

DTNB	5,5′-dithiobis-(2-nitrobenzoic acid)
EGTA	ethylene glycol tetraacetic acid
GSH	reduced glutathione
Nb_{10} ($Nb_{10}O_{28}^{6-}$)	decaniobate
SDS	sodium dodecyl sulphate
SR	sarcoplasmic reticulum
^{51}V-NMR	vanadium-51 NMR
V_1	monomeric vanadate
V_{10} ($V_{10}O_{28}^{6-}$)	decavanadate

Acknowledgements

MA thanks CCMAR; LAEBC and MPMM thank QFM-UC for financial support. CAO is grateful for a QEII fellowship and Discovery Project grant (DP110105530) from the Australian Research Council. WHC acknowledges support from the U.S. Department of Energy Office of Basic Energy Science *via* grant DE-FG02-05ER15693, the National Science Foundation *via* EAR-0814242 and an NSF CCI grant through the Center for Sustainable Materials Chemistry, number CHE-1102637.

References

1 M. Aureliano, T. Tiago, R. M. Gândara, A. Sousa, A. Moderno, M. Kaliva, A. Salifoglou, R. O. Duarte and J. J. J. Moura, *J. Inorg. Biochem.*, 2005, **99**, 2355–2361.
2 M. Aureliano, F. Henao, T. Tiago, R. O. Duarte, J. J. G. Moura, B. Baruah and D. C. Crans, *Inorg. Chem.*, 2008, **47**, 5677–5684.
3 M. Aureliano and V. M. C. Madeira, *Biochim. Biophys. Acta, Mol. Cell Res.*, 1994, **1221**, 259–271.
4 G. Fraqueza, C. A. Ohlin, W. H. Casey and M. J. Aureliano, *J. Inorg. Biochem.*, 2012, **107**, 82–89.
5 B. Schiøtt, M. G. Palmgren, J. V. Møller, P. Nissen and N. Fedosova, *Biochim. Biophys. Acta*, 2009, **1787**, 207–220.
6 T. L. Turner, V. H. Nguyen, C. C. McLauchlan, Z. Dymon, B. M. Dorsey, J. D. Hooker and M. A. Jones, *J. Inorg Biochem.*, 2012, **108**, 96–104.
7 T. Tiago, M. Aureliano and C. Gutierrez-Merino, *Biochemistry*, 2004, **43**, 5551–5561.
8 T. Tiago, P. Martel, C. Gutiérrez-Merino and M. Aureliano, *Biochim. Biophys. Acta*, 2007, **1771**, 474–480.
9 P. Csermely, A. Martonosi, G. C. Levy and A. J. Ejchart, *Biochem. J.*, 1985, **230**, 807–815.
10 S. Hua, G. Inesi and C. Toyoshima, *J. Biol. Chem.*, 2000, **275**, 30546–30550.
11 S. Ramos, M. Manuel, T. Tiago, R. O. Duarte, J. Martins, C. Gutiérrez-Merino, J. J. G. Moura and M. Aureliano, *J. Inorg. Biochem.*, 2006, **100**, 1734–1743.
12 S. Ramos, J. J. G. Moura and M. Aureliano, *J. Inorg. Biochem.*, 2010, **104**, 1234–1239.
13 S. Ramos, R. O. Duarte, J. J. G. Moura and M. Aureliano, *Dalton Trans.*, 2009, 7985–7994.
14 S. Ramos, R. M. Almeida, J. J. G. Moura and M. Aureliano, *J. Inorg. Biochem.*, 2011, **105**, 777–783.
15 S. Ramos, J. J. G. Moura and M. Aureliano, *Metallomics*, 2012, **4**, 16–22.
16 M. Aureliano and D. C. Crans, *J. Inorg. Biochem.*, 2009, **103**, 536–546.
17 M. Aureliano, *Dalton Trans.*, 2009, 9093–9100.
18 L. Yan-Tuan, Z. Chun-Yuan, W. Zhi-Yong, Ma. Jiang and C.-W. Yan, *Transition Met. Chem.*, 2010, **35**, 597–603.
19 F. Zhai, X. Wang, D. Li, H. Zhang, R. Li and L. Song, *Biomed. Pharmacother.*, 2009, **63**, 51–55.

20 V. Dimitrova, K. Zhetcheva and L. P. Pavlova, *J. Chem.*, 2011, **35**, 215–223.
21 A. Zorzano, M. Palacin, L. Marti and S. Garcia-Vicente, *J. Inorg. Biochem.*, 2009, **103**, 559–566.
22 M. J. Pereira, E. Carvalho, J. W. Eriksson, D. C. Crans and M. Aureliano, *J. Inorg. Biochem.*, 2009, **103**, 1687–1692.
23 S. S. Soares, C. Gutiérrez-Merino and M. Aureliano, *J. Inorg. Biochem.*, 2007, **101**, 789–796.
24 S. S. Soares, F. Henao, M. Aureliano and C. Gutierrez-Merino, *Chem. Res. Toxicol.*, 2008, **21**, 607–618.
25 C. A. Ohlin, E. M. Villa and W. H. Casey, *Inorg. Chim. Acta*, 2009, **362**, 1391–1392.
26 C. A. Ohlin, E. M. Villa, J. C. Fettinger and W. H. Casey, *Angew. Chem., Int. Ed.*, 2008, **47**, 8251–8254.
27 S. S. Soares, H. Martins, J. Coucelo, C. Gutiérrez-Merino and M. Aureliano, *J. Inorg. Biochem.*, 2007, **101**, 80–88.
28 B. De Foresta, F. Henao and P. Champeil, *Eur. J. Biochem.*, 1994, **223**, 359–369. 796.
29 K. Fohr, J. Scott, G. Ahnert-Hilger and M. Gratzl, *Biochem. J.*, 1989, **262**, 83–89.
30 L. de Meis and A. L. Vianna, *Annu. Rev. Biochem.*, 1979, **48**, 275–292.
31 D. R. Davies and W. G. J. Hol, *FEBS Lett.*, 2004, **577**, 315–321.
32 G. Inesi, D. Lewis and A. J. Murphy, *J. Biol. Chem.*, 1984, **259**, 996–1003.
33 T. Tiago, M. Aureliano and J. J. G. Moura, *J. Inorg. Biochem.*, 2004, **98**, 1902–1910.
34 D. C. Crans, S. Schoeberl, E. Gaidamauskas, B. Baruah and D. A. Roess, *J. Biol. Inorg. Chem.*, 2011, **16**, 961–972.
35 M. Aureliano, *World J. Biol. Chem.*, 2011, **2**, 215–238.
36 M. B. Colović, D. V. Bajuk-Bogdanovic, N. S. Avramovic, I. D. Holclajtner-Antunovic, N. S. Bošnjaković-Pavlovic, V. M. Vasić and D. Z. Krstić, *Bioorg. Med. Chem.*, 2011, **19**, 7063–7069.
37 P. Csermely, S. Varga and A. Martonosi, *Eur. J. Biochem.*, 1985, **150**, 455–460.
38 S. Varga, P. Csermely and A. Martonosi, *Eur. J. Biochem.*, 1984, **148**, 119–126.
39 R. I. Viner, T. D. Williams and C. Schöneich, *Biochemistry*, 1999, **38**, 12408–12415.
40 T. Tiago, C. Gutiérrez-Merino and M. Aureliano, *Vanadium Biochemistry*, Research Signpost, Kerala, India, 2007, pp. 75–95.
41 D. C. Crans, B. Zhang1, E. Gaidamauskas, A. D. Keramidas, G. R. Willsky and C. R. Roberts, *Inorg Chem.*, 2010, **49**, 4245–4256.
42 R. I. Viner, A. F. Huhmer, D. J. Bigelow and C. Schöneich, *Free Radical Res.*, 1996, **24**, 243–259.
43 D. Jardim-Messeder, J. Camacho-Pereira and A. Galina, *Int. J. Biochem. Cell Biol.*, 2012, **44**, 801–807.
44 C. Toyoshima, M. Nakasako, H. Nomura and H. Ogawa, *Nature*, 2004, **405**, 647–655.
45 P. R. Carey, *Biochemical Applications of Raman and Resonance Raman spectroscopies*, Academic Press, NY, 1982.
46 R. Tuma, *J. Raman Spectrosc.*, 2005, **36**, 307–319.
47 A. Tu, *Raman spectroscopy in Biology*, Wiley and Sons, NY, 1982.
48 Y. Xie, D. Zhang, G. K. Jarori, V. Jo Davisson and D. Ben-Amotz, *Anal. Biochem.*, 2004, **332**, 116–121.
49 M. N. Siamwiza, R. C. Lord and M. C. Chen, *Biochemistry*, 1975, **14**, 4870–4876.
50 Z. Arp, D. Autrey, J. Laane, S. A. Overman and G. J. Thomas, Jr., *Biochemistry*, 2001, **40**, 2522–2529.
51 G. J. Thomas, *Biopolymers (Biospectroscopy)*, 2002, **67**, 214–225.
52 C. H. Nielsen, S. Abdali, J. A. Lundbaek and F. Cornelius, *Spectroscopy*, 2007, **22**, 52–63.
53 A. Amado, M. Aureliano, P. J. Ribeiro-Claro and J. Teixeira-Dias, *J. Raman Spectrosc.*, 1993, **24**, 669–703.